Rheological Model for the Mechanical Properties of Myofibrillar Protein-Based Films

Bernard Cuq,[†] Nathalie Gontard,[‡] Jean Louis Cuq,[§] and Stéphane Guilbert*[,⊥]

Centre de Coopération Internationale en Recherche Agronomique pour le Développement, B.P. 5035, 73 rue J. F. Breton, 34090 Montpellier, France, ENSIA-SIARC, 1101 avenue Agropolis, B.P. 5098, 34033 Montpellier, France, Laboratoire Génie Biologique et Sciences des Aliments, Université de Montpellier II, Place Eugène Bataillon, 34095 Montpellier, France, and Ecole Nationale Supérieure Agronomique de Montpellier, 9 Place Viala, 34060 Montpellier, France

A phenomenological rheological model was developed to describe the molecular interactions and predict the mechanical properties of fish myofibrillar protein-based films, irrespective of their thickness. The model was built of a parallel array of Maxwell and elastic elements in which a fracture element was introduced. The total number of parallel branches was directly correlated with the most characteristic dimension of the samples, *i.e.*, the film thickness. The rheological parameters (α, elastic modulus, and viscosity coefficient) were determined from numerous experimental data sets and appeared to be independent of thickness. They could be used to characterize the molecular interactions in the films. These parameters were only sensitive to the type of data used for calculations (force−deformation, relaxation, or creep) and to the range of experimental conditions applied to obtain these data. The model successfully predicted force−deformation−time relationships for these biopolymer-based films.

Keywords: *Biopolymer film; myofibrillar proteins; mechanical properties; rheological model*

INTRODUCTION

There is now an increasing interest in biodegradable and edible packagings made from entirely renewable natural polymers. The main sources and potential applications of biopolymer films have been recently reviewed by Gontard and Guilbert (1994), Krochta *et al.* (1994), and Cuq *et al.* (1995c). For instance, protein-based films could be used as gas or grease barriers and for mechanical protection in several food systems (Guilbert, 1986, 1988; Aydt *et al.*, 1991; Gennadios *et al.*, 1993b). The mechanical properties of biopolymer films of most natural products are of major importance for many applications. They are usually evaluated by tests involving compression or extension (Gontard *et al.*, 1992; Gennadios *et al.*, 1993a; Hershko *et al.*, 1994) and through interpretation of force−deformation−time relationships (Peleg and Caldaza, 1976; Caldaza and Peleg, 1978). According to Peleg (1977), the conditions under which these tests were performed varied markedly with regard to the specimen dimensions, preconditioning, temperature, relative humidity, magnitude of the force, deformation level, and its application rate.

The mechanical properties of biopolymer films are classically characterized by selective and limited mechanical parameters, such as deformaton or elongation at break, force or strength at break, and relaxation coefficient (Gontard *et al.*, 1993; Stuchell and Krochta, 1994). These mechanical properties are generally influenced both by the type and density of molecular interactions between polymers and by the film thickness (Mahmoud and Savello, 1992; Park *et al.*, 1993; Cuq *et al.*, 1995b). A rheological model, which could on the one hand describe force−deformation−time relationships for this kind of material and on the other hand keep separate the effect of film thickness on mechanical properties, would be then a suitable tool to characterize the molecular interactions occurring in the film matrix.

Empirical models and phenomenological rheological models have been useful tools for evaluating and predicting the mechanical response to force−deformation (or stress−strain) and relaxation kinetics (Peleg, 1979a). Empirical equations were listed by Peleg (1984), and their efficiencies were compared by various authors such as Launay and Cantoni (1987) and Gamero *et al.* (1993). Phenomenological rheological models are often presented in the form of constitutive differential or integral equations relating stress (or force), strain (or deformation) and time or in the form of an electrical circuit or mechanical analog. These models of combined basic elements of linear viscoelasticity [elastic elements, viscous elements and their primary combinations, Maxwell elements (*i.e.*, an in-line array of one elastic element and one viscous element) and Kelvin−Voigt elements (*i.e.*, a parallel array of one elastic element and one viscous element)] are usually applied to describe creep and relaxation data (Peleg, 1979b). The concept of linear viscoelasticity used for these models is only applicable to infinitesimal strain, while strains are in reality finite and sometimes large (Bland, 1960). Models built of 3−10 basic elements are generally sufficient to fit experimental results for a variety of natural products (Peleg, 1976; Chang *et al.*, 1986; Nussinovitch *et al.*, 1989). Special elements can be added to account for phenomena such as plasticity and increased strength (Peleg, 1979b, 1984). Nonlinear responses could be introduced through models with varying numbers of elements (Peleg, 1976; Peleg and

* Author to whom correspondence should be addressed.

[†] Centre de Coopération Internationale en Recherche Agronomique pour le Développement.

[‡] ENSIA-SIARC.

[§] Université de Montpellier II.

[⊥] Ecole Nationale Supérieure Agronomique de Montpellier.

0021-8561/96/1444-1116$12.00/0

Normand, 1982). The irreversible nature of food deformation can be represented by rheological models that contain elements with fracture components (Drake, 1971; Peleg, 1976). The usual characteristic parameters of these rheological models (*e.g.*, elastic modulus, viscosity) have already been calculated through experimental data fitting to quantify the mechanical behavior of natural products (Chang *et al.*, 1986; Gamero *et al.*, 1993).

The mechanical properties of myofibrillar protein-based films were previously studied to determine force−deformation curves and relaxation kinetics at various film thicknesses (Cuq *et al.*, 1995b). It has been shown that a film thickness increase involved significant modifications in mechanical properties due to an increase in the number of protein chains per surface unit. The type and density of molecular interactions were found to be independent of the film thickness. From these experiments, it appears that the study of the effect of specific parameters such as plasticizer content on the type and density of molecular interactions does then require either working only with films of the same thickness or keeping separate the effect of film thickness on the measured variations of mechanical properties. In the present study, a phenomenological rheological model is proposed to characterize the molecular interactions in myofibrillar protein-based films, irrespective of the film thickness.

MATERIALS AND METHODS

Preparation of Fish Mince. Washed fish mince was prepared from Atlantic sardines according to the method of Cuq *et al.* (1995a). Gutted and headed fish were passed through a meat bone separator, washed with water, strained in a rotary rinser, passed through a refiner, and chopped in a cutter. The fish mince was vacuum packed and kept at −23 °C. Samples were thawed for 24 h at 4 °C before experiments.

Preparation of Myofibrillar Protein-Based Films. Films were prepared from a film-forming solution (FFS) based on fish mince in distilled water and acetic acid. Protein concentration (2.0 g/100 g of FFS), pH (3.0), and glycerol concentration (35 g/100 g of dry matter) were adjusted from those of Cuq *et al.* (1995a). All components were mixed at 25 °C in a vacuum homogenizer (Stephan UM5, Marne la Vallée, France). FFS were stored for 6 h before casting on a PVC plate using a thin-layer chromatography spreader. The film thickness variations were obtained by modifying the "apparent thickness" of the cast FFS. The thin layer of FFS was dried in a ventilated oven at 25 °C for about 10−24 h. Transparent films were thus formed. Films were equilibrated at 59.1% relative humidity (using a saturated aqueous NaBr solution) and 20 °C for 48 h before testing.

Characterization of Myofibrillar Protein-Based Films. Thickness was measured with a hand-held micrometer (Braive Instruments, Checy, France) with 7.5 mm diameter faces to the nearest 10^{-6} m. Thickness values are means of 10 measurements.

The mechanical properties were determined at 20 °C and 59.1% relative humidity using a SMS Stable microsystem TA-XT2 rheometer (Champlan, France), operated according to a method described by Bourne (1968). This method is particularly well adapted to biopolymer films. Samples preset on measuring clamps are analyzed without any handling, thus limiting potential transfers from the environment. Moreover, measurements are not sensitive to possible edge effects. Films were cut into 40 mm diameter disks and fixed in an annular ring clamp (34 mm diameter). A cylindrical probe (3 mm diameter) was displaced perpendicularly to the film surface at constant speed (0.5 mm s^{-1}). From the probe displacement, the film deformation was calculated as follows, where $L(t)$ is the deformation (m), $D(t)$ is the probe displacement (m), R_0 is the initial film length (15.5 mm), and t is the time (s):

$$L(t) = \sqrt{D(t)^2 + R_0^2} - R_0^2 \quad (1)$$

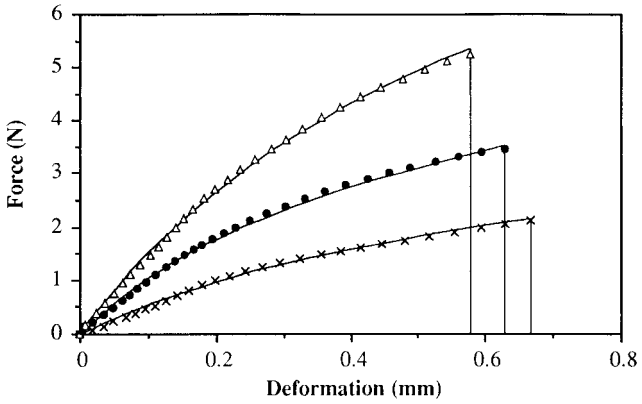

Figure 1. Experimental force−deformation data recorded under a constant rate of deformation (0.072 mm s^{-1}) for myofibrillar protein-based films. Thickness is 17 (×), 39 (●), or 54 μm (△), where (—) are the fitted curves, calculated with eq 13.

Experiments were carried out to determine force−deformation, relaxation, and creep curves. Force (N)−deformation (m) curves were plotted until the probe passed through the film. Although the deformation rate was slightly dependent on the extent of deformation, we have considered that it is equivalent to the average deformation rate throughout the experiment (V = 0.072 mm s^{-1}). Relaxation tests were carried out after 0.29 mm of deformation. This deformation was maintained for 60 s and force (N)−time (s) curves were plotted. Creep tests were carried out under constant force (0.5, 1.0, 1.5, or 2.0 N), and deformation (m)−time (s) curves were plotted for 60 s.

Mathematical Calculations. The critical fracture deformations (L_C) were directly determined from experimental deformation at break values. The three parameters of the model (α, K, and η) were identified from force−deformation data sets with eq 13, from relaxation data sets with eq 16, and from creep data sets with eq 21. The three parameters were calculated by an optimization procedure according to the Gauss−Newton algorithm (Trigeassou, 1988). The minimized objective function was the sum of residuals squared (*i.e.* deviations between experimental and predicted points).

RESULTS AND DISCUSSION

Model Establishment: Theoretical Considerations. The mechanical properties of myofibrillar protein-based films (*i.e.*, typical force−deformation curves, relaxation kinetics, and creep kinetics) are represented for various thicknesses in Figures 1−3 (Cuq *et al.*, 1995b).

Among linear rheological models (Courraze and Grossiord, 1991), the generalized Maxwell model for solid materials (*i.e.*, a parallel array of a number of Maxwell elements with one elastic element) is able to describe the shapes of the curves presented in Figures 1−3. This kind of model is well adapted to describe the nonlinear force−deformation relationship (Figure 1), the residual force remaining after a long relaxation time (Figure 2), and the finite strain after a long creep time (Figure 3). Nevertheless, this conventional model cannot account for the actual rheological behavior of myofibrillar protein-based films and in particular for the effect of film thickness. This model has then been modified to meet the following conditions:

(1) To describe the failure phenomena in force−deformation curves (Figure 1), each element in parallel

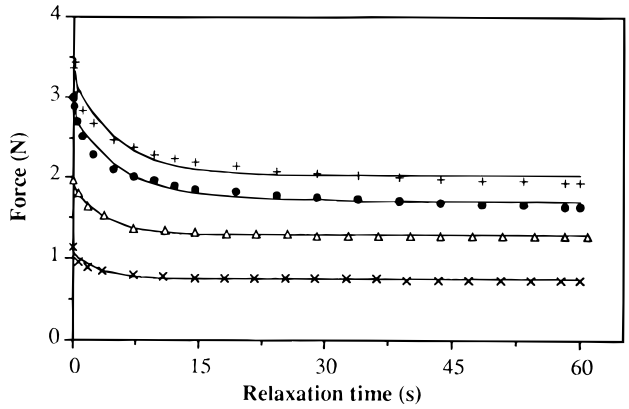

Figure 2. Experimental relaxation data (constant deformation = 0.29 mm) for myofibrillar protein-based films. Thickness is 12 (×), 27 (△), 36 (●), or 49 μm (+), where (—) are the fitted curves, calculated with eq 16.

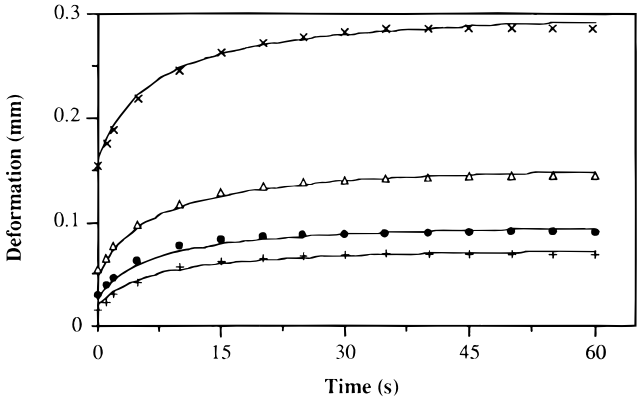

Figure 3. Experimental creep data (constant force = 1 N) for myofibrillar protein-based films. Thickness is 13 (×), 25 (△), 39 (●), or 51 μm (+), where (—) are the fitted curves, calculated with eq 21.

(*i.e.*, Maxwell or elastic elements) is modified by the in-line incorporation of a fracture element. Force peaks followed by instantaneous drops are then anticipated (Drake, 1971). The fracture elements behave as rigid elements before failure. Once its force level is reached (critical fracture force, F_C), the element is dissected.

(2) To describe the effect of film thickness on mechanical properties observed in Figures 1−3 and in particular on the residual force remaining after a long relaxation time (Figure 2), more than one elastic element is added in parallel to the Maxwell elements.

(3) To keep separate the effect of molecular interactions occurring in the film, the total number of parallel branches (N_G) of the model is correlated with the film thickness. The simplest relationship is proposed, whereby N_G is supposed equal to the film thickness (expressed in micrometers).

(4) To set a simple description of the molecular interactions in film, the characteristics of the elastic, viscous, and fracture elements are supposed to be the same irrespective of their position in the model.

The model proposed to describe mechanical properties of the myofibrillar protein-based films is presented in Figure 4. As the calculation of stress loads from the experimental results of Cuq *et al.* (1995b) is of considerable complexity, the following relationships and calculations are based on force units (N). The elastic and viscous elements of the model are characterized by elastic modulus K (N m^{-1}) and viscosity η (N s m^{-1}), respectively (Peleg, 1976). The fracture elements are characterized by critical fracture forces: F_{CE} (N) when associated with elastic elements and F_{CM} (N) when associated with Maxwell elements. It is usual to define critical fracture deformation by the deformation at critical fracture force (Peleg, 1976). To describe the abrupt drop in force at the break point, we hypothesize that the critical fracture deformations at F_{CE} or F_{CM} are equal (L_C, m).

The total number of parallel branches (N_G) is defined by the sum of the number (N_E) of branches including an elastic element and the number (N_M) of branches including a Maxwell element (eq 2). N_E and N_M are correlated with N_G by eqs 3 and 4.

$$N_G = N_E + N_M \tag{2}$$

$$N_E = \alpha N_G \tag{3}$$

$$N_M = (1 - \alpha)N_G \tag{4}$$

α is the proportion of parallel branches including an elastic element. According to Peleg (1976), for a parallel array of branches, the total force is the sum of the forces acting on each branch (eq 5).

$$F = \sum_{i=1}^{N_E} F_i + \sum_{j=1}^{N_M} F_j \tag{5}$$

F is the total force (N), F_i is the force (N) acting on a branch including an elastic element, and F_j is the force (N) acting on a branch including a Maxwell element.

As the characteristics of the elements are supposed to be the same irrespective of their position in the model, eq 5 becomes

$$F = \alpha N_G F_i + (1 - \alpha)N_G F_j \tag{6}$$

According to Peleg (1976), for a parallel array of branches, once deformation has commenced, it is the same for all individual parallel branches (eq 7).

$$L(t) = L_i(t) = L_j(t) \tag{7}$$

$L(t)$ is the deformation (m), $L_i(t)$ is the deformation (m) of a parallel branch (i) including an elastic element, $L_j(t)$ is the deformation (m) of a parallel branch (j) including a Maxwell element, and t is the time (s).

According to Peleg (1976) and Couarraze and Grossiord (1991), the general force−deformation relationships of an elastic element and a viscous element are described by eqs 8 and 9, respectively.

$$F = KL \tag{8}$$

$$dL/dt = F/\eta \tag{9}$$

The general force−deformation relationship (eq 10) of a Maxwell element (*i.e.*, an in-line array of an elastic and a viscous element) is simply established from eqs 8 and 9:

$$\frac{dL}{dt} = \frac{1}{K}\frac{dF}{dt} + \frac{F}{\eta} \tag{10}$$

K is the elastic modulus (N m^{-1}) of an elastic element and η is the viscosity (N s m^{-1}) of a viscous element.

Force−Deformation Relationships under a Constant Rate of Deformation. When a constant rate of deformation is applied, the force−deformation relationships of an elastic element (eq 11) and a Maxwell element (eq

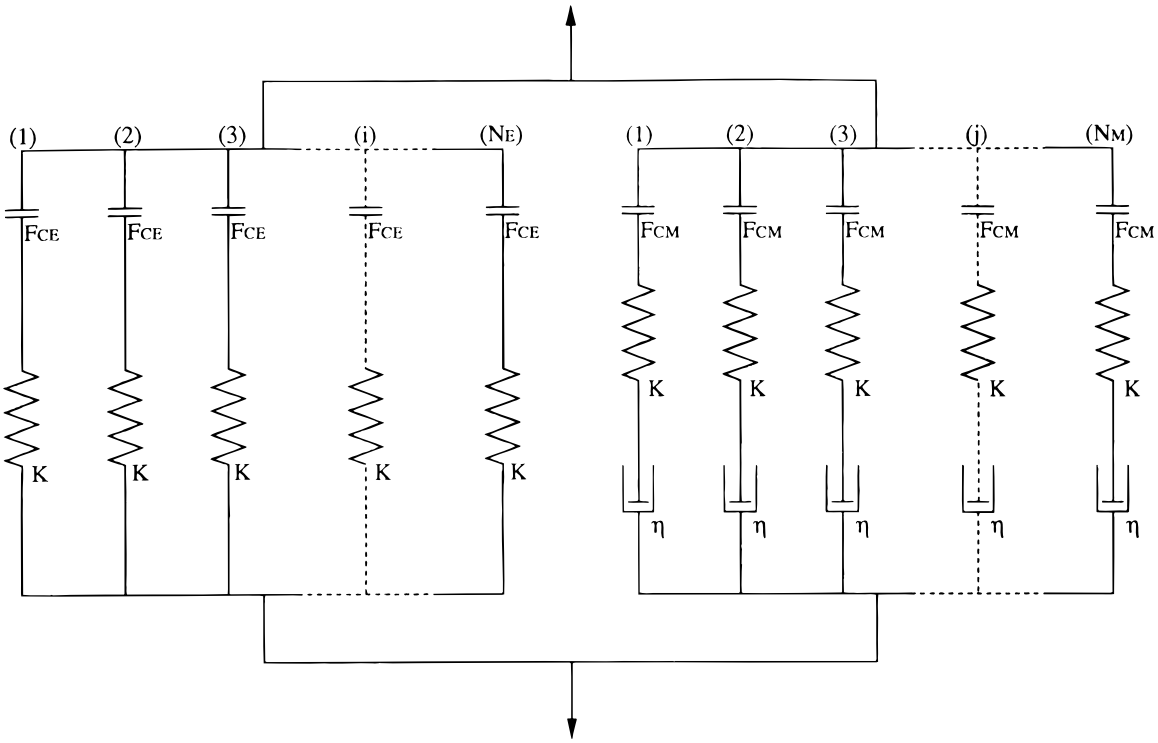

Figure 4. Schematic representation of the model established to describe the mechanical properties of the myofibrillar protein-based films. N_E and N_M are the number of branches including an elastic element (*i*) or a Maxwell element (*j*), K is the elastic modulus (N m^{-1}) for the elastic elements, L_C is critical fracture deformation (m) for the fracture elements, and η is the viscosity (N s m^{-1}) for the viscous elements.

12) are established from eqs 8 and 10, with the following initial conditions: $t = 0$, $F(0) = 0$, and $L(0) = 0$.

$$F_i(L) = KL \tag{11}$$

$$F_j(L) = \eta V\left[1 - \exp\left(-\frac{KL}{\eta V}\right)\right] \tag{12}$$

V is the constant rate of deformation [$V = dL/dt = L(t)/t$]. From eqs 6, 11, and 12, the force−deformation relationship of the model (eq 13) is then established, when $L < L_C$.

$$F(L) = \alpha N_G KL + (1 - \alpha)N_G \eta V\left[1 - \exp\left(-\frac{KL}{\eta V}\right)\right] \tag{13}$$

Force−Time Relationships (Relaxation Kinetics). For relaxation tests when deformation remains constant (L_R), the force−time relationships of an elastic element (eq 14) and a Maxwell element (eq 15) are established from eqs 8 and 10, with the following initial conditions: $t = 0$, $L(0) = L_R$.

$$F_i(t) = KL_R \tag{14}$$

$$F_j(t) = \eta V\left[1 - \exp\left(-\frac{KL_R}{\eta V}\right)\right]\exp\left(-\frac{Kt}{\eta}\right) \tag{15}$$

L_R is the constant deformation for the relaxation test. The force−time relationship of the model (eq 15) is then established from eqs 6, 14, and 15, when $L_R < L_C$.

$$F(t) = \alpha N_G KL_R + (1 - \alpha)N_G \eta V\left[1 - \exp\left(-\frac{KL_R}{\eta V}\right)\right] \times \exp\left(-\frac{Kt}{\eta}\right) \tag{16}$$

Deformation−Time Relationships (Creep Kinetics). For creep tests when force remains constant (F_{creep}), the deformation−time relationships of an elastic element (eq 17) and a Maxwell element (eq 18) are established from eqs 8 and 10, with the following initial conditions: $t = 0$, $F(0) = F_{creep}$, and $L(0) = L_{creep}$.

$$F_i(t) = KL(t) \tag{17}$$

$$F_j(t) = [(L(t) - L_{creep})\eta]/t \tag{18}$$

F_{creep} is the constant force for the creep tests and L_{creep} is the initial deformation at F_{creep}. The deformation−time relationship of the model (eq 21) is established from eqs 6, 14, and 15, until $L(t) < L_{creep}$ (eqs 19 and 20 are intermediate equations).

$$F_{creep} = \alpha N_G F_i(t) + (1 - \alpha)N_G F_j(t) \tag{19}$$

$$F_{creep} = \alpha N_G KL(t) + (1 - \alpha)N_G \frac{(L(t) - L_{creep})\eta}{t} \tag{20}$$

$$L(t) = \frac{F_{creep}t + (1 - \alpha)N_G \eta L_{creep}}{\alpha N_G Kt + (1 - \alpha)N_G \eta} \tag{21}$$

Equations 13, 16, and 21 describe the force−deformation−time relationships of the model. It should be mentioned that four parameters (K, η, α, and L_C) in the model could be used to describe the molecular interactions of the films. According to Bland (1960), the concepts of linear viscoelasticity used in the phenomenological model are only applicable to infinitesimal strain. In reality the strains are finite; for instance, the strain at break is 4.9% for myofibrillar protein-based films (Cuq *et al.*, 1995b). Nevertheless, even if the applied strain level is in most cases out of the linear viscoelastic domain, the use of eqs 13, 16, and 21, which

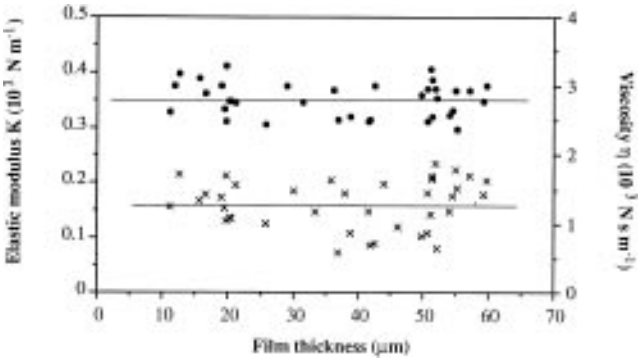

Figure 5. Effect of film thickness on the values of elastic modulus K (●) and viscosity η (×) calculated with eq 13 from experimental force−deformation data for the myofibrillar protein-based films.

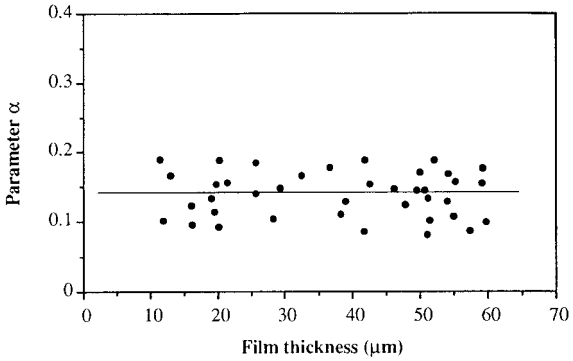

Figure 6. Effect of film thickness on the values of parameter α calculated with eq 13 from experimental force−deformation data for the myofibrillar protein-based films.

are based on phenomenological considerations, is no more than a mathematical fitting process.

Fit of the Model. The three parameters of the model (α, K, and η) are calculated to fit experimental data for myofibrillar protein-based films of various thicknesses. Preliminary calculations have shown that in the possible range of these three parameters, $\alpha = 0-1$, $K = 1-10^5$ N m^{-1}, and $\eta = 1-10^4$ N s m^{-1}, the objective function is characterized by only one main minimum. A single combination of the parameters (α, K, and η) can thus be used to fit with precision the experimental force−deformation, relaxation, and creep data. Typical fits of the model to experimental data are presented in Figures 1−3. As a general rule, the model has about the same degree of fit and the fitted curves are practically indistinguishable from the experimental data regardless of the film thickness.

Effect of Film Thickness. The originality of the model presented by eqs 13, 16, and 21 resides in its possibility to keep separate the effect of thickness on the mechanical properties of films. The parameters (α, K, and η) are calculated from the whole experimental data sets that were established with film thicknesses between 10 and 60 μm (Cuq *et al.*, 1995b). The effects of the film thickness on the values of the parameters K and η (Figure 5) and α (Figure 6) are represented when calculations are carried out from force−deformation data. The effects of thickness are similar when the parameters are calculated from relaxation or creep data. As expected, the values for the parameters (α, K, and η) are not significantly influenced by thickness variations. Mean values of the parameters can be calculated for these films, irrespective of their thickness.

According to Cuq *et al.* (1995b), the critical fracture deformation of the fracture elements introduced in each parallel branch of the model (Figure 4) appears to be

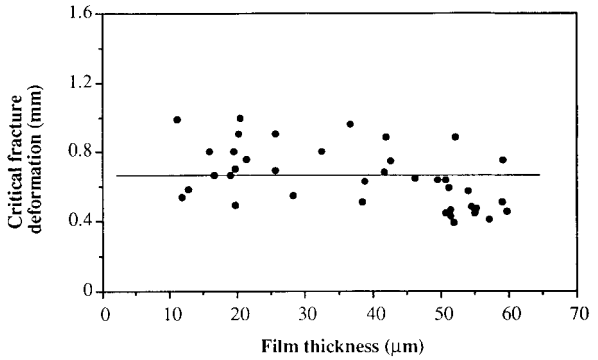

Figure 7. Effect of film thickness on the values of critical fracture deformation calculated from experimental force−deformation data for the myofibrillar protein-based films.

independent of the film thickness (Figure 7). The relative lack of precision observed could be associated with experimental error as already noted with data measurements (Cuq *et al.*, 1995b).

As expected, variations in the total number (N_G) of parallel branches in the model govern the effect of film thickness on mechanical properties. The relationship that has been proposed to correlate film thickness and the total number of parallel branches (*i.e.*, N_G is supposed equal to film thickness expressed in micrometers) is then valid. The parameters (α, K, and η) and the critical fracture deformation can then be used to characterize the molecular interactions in biopolymer films, irrespective of their thickness. For instance, the elastic modulus (K) is a fundamental measure of film stiffness and can characterize the reversibility properties of molecular interactions, while the viscosity (η) is an indicator of the density of molecular interactions.

Limitations of the Model. The parameters appear to be influenced by the type of data (force−deformation, relaxation, or creep) used for calculations (Table 1). For the parameters calculated to describe the mechanical properties of myofibrillar protein-based films, viscosity is equal to 1260 N s m^{-1} when calculations are made from force−deformation data, 1520 N s m^{-1} when calculations are made from relaxation data, and 3400 N s m^{-1} when calculations are made from creep data. Similar variations are observed with the parameters α and K.

Conditions applied to determination of experimental data also affected the calculated values of the parameters (K, α, and η). For instance, the parameters calculated from creep tests under various levels of forces (Table 2) are sensitive to the range of experimental conditions: when $F_{creep} = 0.5$ N, $K = 580$ N m^{-1} and $\eta = 3000$ N s m^{-1}, while $K = 430$ N m^{-1} and $\eta = 5400$ N s m^{-1} when $F_{creep} = 2.0$ N. Such behaviors have been found when the initial deformation (Peleg, 1979a) or deformation rate (Peleg and Calzada, 1976) changed for relaxation tests and when the initial force changed for creep tests (Chang *et al.*, 1986). In these conditions, comparisons of the model parameters for various materials have to be made with values calculated from the same kind of experimental data obtained under the same conditions.

Two hypotheses are proposed to explain this relative sensitivity of the model: (i) the model does not take into consideration the continuous internal fractures that potentially occur in these biopolymer films, while the samples apparently remained intact (Pollack and Peleg, 1980), and (ii) the model is applied out of linear viscoelasticity range where the phenomenological models are defined.

Table 1. Calculated Values[a] of the Rheological Parameters Determined from Force−Deformation, Relaxation, or Creep Data Fits with Equations 13, 16, and 21, Respectively

films	type of data	rheological parameters			
		α	K (N m^{-1})	η (N s m^{-1})	L_C (mm)
myofibrillar protein	force−deformation	0.15 (0.05)	350 (40)	1260 (300)	0.65 (0.18)
	relaxation kinetics	0.50 (0.02)	335 (25)	1520 (70)	
	creep kinetics	0.50 (0.20)	500 (90)	3400 (900)	
cellulose	force−deformation	1	140 (20)		2.32 (0.12)
LDPE	force−deformation	0	510 (60)	1950 (220)	3.30 (0.68)

[a] Standard deviations are given in parentheses. K is the elastic modulus, L_C is the critical fracture deformation, LDPE is low-density polyethylene, α is a model parameter, and η is the viscosity.

Table 2. Effect of the Creep Force Level on Values[a] of the Parameters α, *K*, and η Calculated with Equation 21 from Creep Data for Myofibrillar Protein-Based Films

constant force (N)	rheological parameters		
	α	K (N m^{-1})	η (N s m^{-1})
0.5	0.5 (0.2)	580 (120)	3000 (1000)
1.0	0.5 (0.2)	500 (90)	3400 (900)
1.5	0.5 (0.2)	420 (150)	3200 (800)
2.0	0.5 (0.2)	430 (110)	5400 (1100)

[a] Standard deviations are given in parentheses. α is a model parameter, K is the elastic modulus, and η is the viscosity.

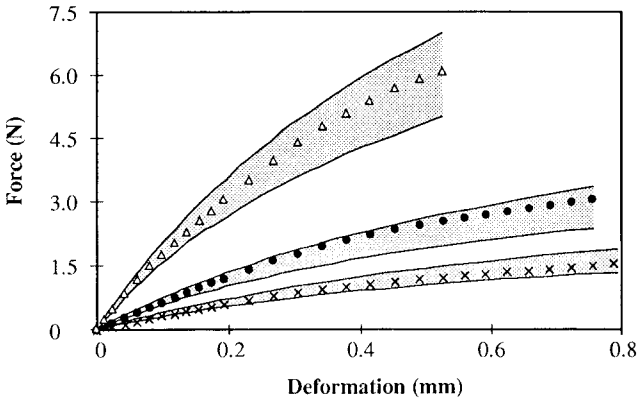

Figure 8. Model validation: comparison between independent force−deformation data of myofibrillar protein-based films. Thickness is 11 (×), 21 (●), or 59 μm (△); the predicted curves (—) from the minimum values (α = 0.1, K = 310 N m^{-1}, η = 960 N s m^{-1}) or maximum values (α = 0.2, K = 390 N m^{-1}, η = 1560 N s m^{-1}) of parameters were calculated with eq 13, where the shading represents the predicted surface.

Comparison with Other Films. The calculated parameters for myofibrillar protein-based films can be compared with those for cellulose or low-density polyethylene-based films (Table 1). Calculations are based on force−deformation data registered under the same experimental conditions. The cellulose-based films are characterized by an elastic behavior (α = 1), and polyethylene-based films behave like a Maxwell material (α = 0). According to the preceding results, these values of α cannot be applied to calculate relaxation or creep curves.

These two materials are characterized by very large critical deformations (L_C = 2.32 and 3.3 mm for cellulose- and polyethylene-based films, respectively) as compared to myofibrillar protein-based films (L_C = 0.65 mm). Comparison of elastic modulus values shows that interactions occurring in protein-based films (K = 350 N m^{-1}) seem to be more reversible than those in cellulose-based films (K = 135 N m^{-1}) but less reversible than those in polyethylene-based films (K = 510 N m^{-1}).

Prediction by the Rheological Model. The proposed model can be used to predict force−deformation, relaxation curves, or creep curves of films as a function of thickness. To take the observed relative lack of precision into consideration, minimum and maximum values of the three parameters are calculated (mean ± standard deviation). They are used to calculate minimum and maximum fitted curves so that experimental data are included in a predicted surface. Figures 8 and 9 present independent experimental data and the corresponding predicted surface for force−deformation curves and relaxation kinetics, respectively. Similar results were observed with creep curves. The model is able to predict the rheological behavior for myofibrillar protein-based films because the independent data are included in the predicted surface irrespective of the film thickness.

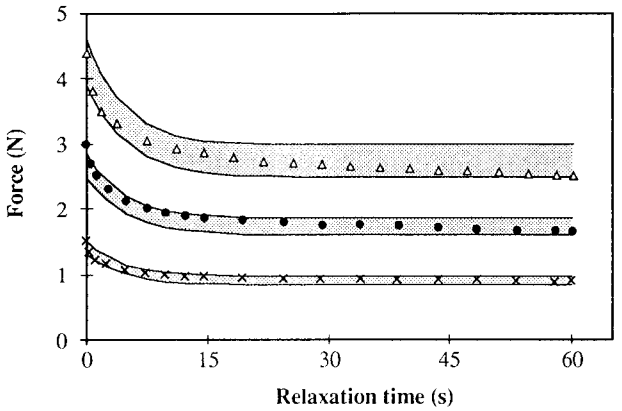

Figure 9. Model validation: comparison between independent force−deformation data of myofibrillar protein-based films. Thickness is 21 (×), 36 (●), or 57 μm (△); the predicted curves (—) from the minimum values (α = 0.5, K = 310 N m^{-1}, η = 1450 N s m^{-1}) or maximum values (α = 0.5, K = 360 N m^{-1}, η = 1590 N s m^{-1}) of parameters were calculated with eq 16, where the shading represents the predicted surface.

ACKNOWLEDGMENT

We thank Christian Aymard (Université de Montpellier II, Laboratoire de Chimie Biomoléculaire, Place Eugène Bataillon, 34095, Montpellier, France) for valuable advice and help.

NOMENCLATURE

$D(t)$	probe displacement (m)
$F(L)$, $F(t)$	force (N)
F_{CE}	critical fracture force (N) of a fracture element when associated with an elastic element
F_{CM}	critical fracture force (N) of a fracture element when associated with a Maxwell element
F_{creep}	constant force (N) for the creep test
$F_i(L)$, $F_i(t)$	force acting (N) on a branch (i) including an elastic element
$F_j(L)$, $F_j(t)$	force acting (N) on a branch (j) including a Maxwell element
i	position in the model of a branch including an elastic element

j	position in the model of a branch including a Maxwell element
K	elastic modulus (N m^{-1})
$L(t)$	deformation (m)
L_C	critical fracture deformation (m)
L_{creep}	initial deformation (m) at the constant force for the creep test
$L_i(t)$	deformation (m) of a branch (i) including an elastic element
$L_j(t)$	deformation (m) of a branch (j) including a Maxwell element
L_R	constant deformation (m) for the relaxation test
N_E	number of branches of the model including an elastic element
N_G	total number of parallel branches of the model
N_M	number of branches of the model including a Maxwell element
R_0	initial film length (m)
t	time (s)
V	rate of deformation (m s^{-1})
α	proportion of branches in the model including an elastic element
η	viscosity (N s m^{-1})

LITERATURE CITED

Aydt, T. P.; Weller, C. L.; Testin, R. F. Mechanical and barrier properties of edible corn and wheat protein films. *Trans. ASAE* **1991**, *34*, 207−211.

Bland, D. R. *The Theory of Linear Viscoelasticity*; Pergamon Press: London, 1960.

Bourne, M. C. Texture profile of ripening pears. *J. Food Sci.* **1968**, *33*, 223−226.

Caldaza, J. F.; Peleg, M. Mechanical interpretation of compressive stress-strain relationship of solid foods. *J. Food Sci.* **1978**, *43*, 1087−1092.

Chang, Y. S.; Guo, T. A.; Lee, Y. P.; Sperling, L. H. Viscoelasticity of cheese. *J. Food Sci.* **1986**, *63*, 1077−1078.

Couarraze, G., Grossiord, J. C., Eds. *Introduction to Rheology*, 2nd ed.; Technique et Documentation, Lavoisier; Apria: Paris, 1991.

Cuq, B.; Aymard, C.; Cuq, J. L.; Guilbert, S. Edible packaging films based on fish myofibrillar proteins: formulation and functional properties. *J. Food Sci.* **1995a**, in press.

Cuq, B.; Gontard, N.; Cuq, J. L.; Guilbert, S. Influence of film thickness on functional properties of myofibrillar protein-based biopackagings. *J. Food Sci.* **1995b**, in press.

Cuq, B.; Gontard, N.; Guilbert, S. Edible films and coatings as active layers. In *Active Food Packagings*; Rooney, M. L., Ed.; Blackie Academic & Professional: Glasgow, 1995c; pp 111−142.

Drake, B. A quasi-rheological model element for fracture. *J. Texture Stud.* **1971**, *2*, 365−372.

Gamero, M.; Fiszman, S. M.; Duran, L. Stress relaxation of fruit gels. Evaluation of models and effects of composition. *J. Food Sci.* **1993**, *58*, 1125−1128.

Gennadios, A.; Park, H. J.; Weller, C. L. Relative humidity and temperature effects on tensile strength of edible protein and cellulose ether films. *Trans. ASAE* **1993a**, *36*, 1867−1872.

Gennadios, A.; Weller, C. L.; Testin, R. F. Temperature effect on oxygen permeability of edible protein-based films. *J. Food Sci.* **1993b**, *58*, 212−219.

Gontard, N.; Guilbert, S. Bio-packaging: technology and properties of edible and/or biodegradable material of agricultural origin. In *Food Packaging and Preservation*; Mathlouthi, M., Ed.; Blackie Academic & Professional: Glasgow, 1994; pp 159−181.

Gontard, N.; Guilbert, S.; Cuq, J. L. Edible wheat gluten films: influence of the main process variables on film properties using response surface methodology. *J. Food Sci.* **1992**, *57*, 190−195, 199.

Gontard, N.; Guilbert, S.; Cuq, J. L. Water and glycerol as plasticizers affect mechanical and water vapor barrier properties of an edible wheat gluten film. *J. Food Sci.* **1993**, *58*, 206−211.

Guilbert, S. Technology and application of edible protective films. In *Food Packaging and Preservation, Theory and Practice*; Mathlouthi, M., Ed.; Elsevier Applied Science Publishers: London, 1986; pp 371−394.

Guilbert, S. Use of superficial edible layer to protect intermediate moisture foods: application to the protection of tropical fruit dehydrated by osmosis. In *Food Preservation by Moisture Control*; Seow, C. C., Teng, T. T., Quah, C. H., Eds.; Elsevier Applied Science Publishers: London, 1988; pp 199−219.

Hershko, V.; Rabinowitch, H. D.; Nussinovitch, A. Tensile characteristics of ripe tomato skin. *Lebensm. Wiss. Technol.* **1994**, *27*, 386−389.

Krochta, J. M., Baldwin, E. A., Nisperos-Carriedo, M., Eds. *Edible Films and Coatings to Improve Food Quality*; Technomic Publishing: Lancaster, PA, 1994.

Launay, B.; Cantoni, P. Interpretation of stress relaxation curves: some theoritical and practical aspects. In *Physical Properties of Foods*; Sowitt, R., Ed.; Elsevier Applied Science Publishers: London, 1987; pp 455−470.

Mahmoud, R.; Savello, P. A. Mechanical properties of and water vapor transferability through whey protein films. *J. Dairy Sci.* **1992**, *75*, 942−946.

Nussinovitch, A.; Peleg, M.; Normand, M. D. A modified Maxwell and a nonexponential model for characterization of the stress relaxation of agar and alginate gels. *J. Food Sci.* **1989**, *54*, 1013−1016.

Park, H. J.; Weller, C. L.; Vergano, P. J.; Testin, R. F. Permeability and mechanical properties of cellulose-based edible films. *J. Food Sci.* **1993**, *58*, 1361−1364, 1370.

Peleg, M. Considerations of a general rheological model for the mechanical behavior of viscoelastic solid food materials. *J. Texture Stud.* **1976**, *7*, 243−255.

Peleg, M. The role of the specimen dimensions in uniaxial compression of food materials. *J. Food Sci.* **1977**, *42*, 649−659.

Peleg, M. Characterization of the stress relaxation curves of solid foods. *J. Food Sci.* **1979a**, *44*, 277.

Peleg, M. Rheological model for solid foods. In *Food Process Engineering*; Linko, P., Mälki, Y., Olkku, J., Larinkari, J., Eds.; Food Processing Systems: 1979b; pp 250−256.

Peleg, M. Application of nonlinear phenomenological rheological models to solid biomaterials. *J. Texture Stud.* **1984**, *15*, 1−22.

Peleg, M.; Caldaza, J. F. Stress relaxation of deformed fruits and vegetables. *J. Food Sci.* **1976**, *41*, 1325−1329.

Peleg, M.; Normand, M. D. A computer assisted analysis of some theoritical rate effects in mastication and in deformation testing of foods. *J. Food Sci.* **1982**, *47*, 1572−1578.

Pollack, N.; Peleg, M. Early indications of failure in large compressive deformation of solid foods. *J. Food Sci.* **1980**, *45*, 825−830.

Stuchell, Y. M.; Krochta, J. M. Enzymatic treatments and thermal effects on edible soy protein films. *J. Food Sci.* **1994**, *59*, 1332−1337.

Trigeassou, J. C. *Recherche de Modèles Expérimentaux Assistée par Ordinateur*; Technique et Documentation Language et Informatique, Lavoisier, Apria: Paris, 1988.

Received for review June 26, 1995. Revised manuscript received November 2, 1995. Accepted February 1, 1996.[⊗] This research was supported by a grant from the Ministère de l'Enseignement Supérieur et de la Recherche (Contrat Aliment 2002, 92.G.0672, 11/18/92).

JF950389N

[⊗] Abstract published in *Advance ACS Abstracts,* March 15, 1996.